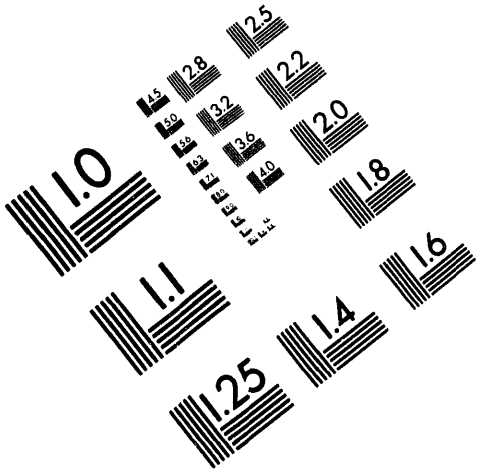

**Association for Information and Image Management**
1100 Wayne Avenue, Suite 1100
Silver Spring, Maryland 20910
301/587-8202

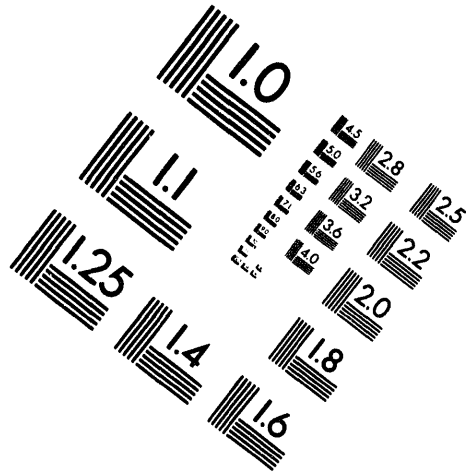

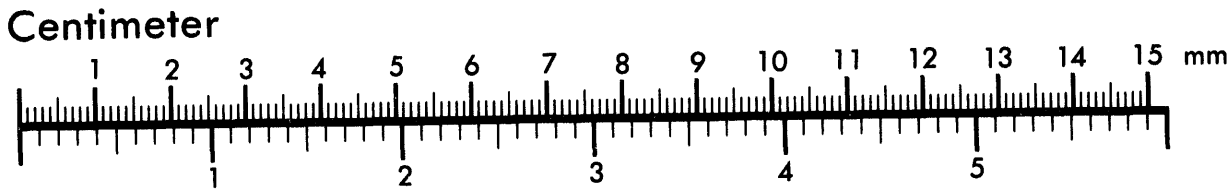


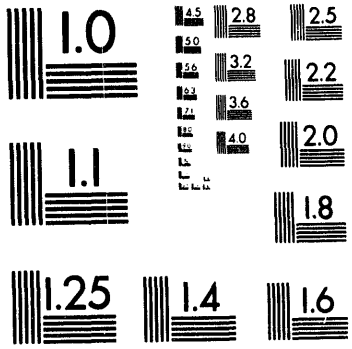

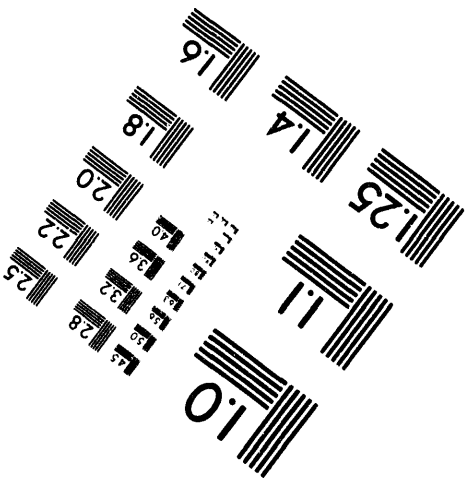

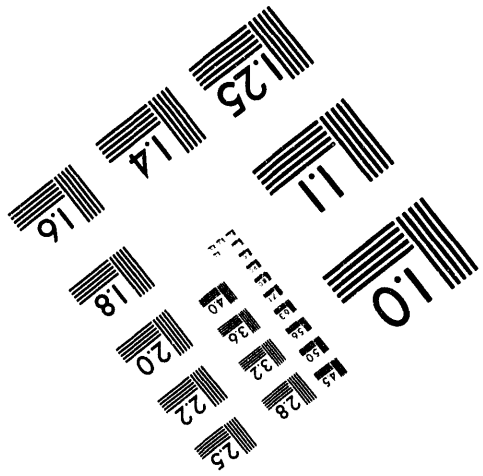

1 of 1

SAND94-1239C
Conf-940552--6

# PBFA II LITHIUM BEAM CHARACTERIZATION FROM INNER-SHELL X-RAY IMAGES

**A. R. Moats, M. S. Derzon, G. A. Chandler, R. J. Dukart, T. A. Haill**

**Sandia National Laboratories**

**P. O. Box 5800**

**Albuquerque, New Mexico 87185**



The Particle Beam Fusion Accelerator (PBFA II) is now driving targets with ICF-relevant lithium ion beams. During the most recent lithium beam target series, time-integrated x-ray pinhole cameras viewed the ion-induced inner-shell x-ray fluorescence from the central gold cone target and a titanium-coated strip. Ion beam profiles at a nominal 10 mm radius and fixed azimuthal direction were obtained from images of the Ti $K_\alpha$ fluorescence of a Ti-coated Al diagnostic wire. The gold cone gave us beam profiles at a nominal 3 mm radius and at all azimuthal angles from the Au $L_\alpha$ fluorescence. From these profiles, we obtained the ion beam vertical focus position, full-width-at-half-maximum, and the degree of azimuthal uniformity for the lithium target shots. For these initial results, beam steering problems were evident. Azimuthal uniformity was measured from the ion beam footprint on the outer Au case (predominantly Au $L_\alpha$) of the hohlraum target and were found to be in the same range (up to 30%) as for previous proton beam target series. We then present plans for Li beam diagnostics for an upcoming target experimental series.

## I. Introduction

The Particle Beam Fusion Accelerator (PBFA II) at Sandia National Laboratories is being used to explore inertial confinement fusion (ICF) physics with lithium ion beams as the fusion driver. PBFA II employs an applied-B ion diode in a cylindrical (or barrel) geometry to accelerate either proton or lithium ion beams from the outer anode and then focus these ions radially inward to the center target. The details of the PBFA II diode design are discussed elsewhere.[1-3] For our initial lithium-beam target series presented here, ~ 20 kJ of 9 MeV lithium ions were focussed for a 15 ns pulse on a nominal 6 mm sphere centered at the diode.[4]

The experimental series discussed here was our first set of experiments studying beam deposition and foam opacity in a hohlraum target in a lithium ion beam. Achieved target temperature during the present experiment is not greatly affected by beam symmetry, since temperature at these ion intensities is due to total ion energy loss within the target. However, we need to characterize the present ion beam for input into our predictive codes, to expand our data base of ion beam behavior, and to prepare to future high convergence experiments when beam symmetry will play a more important role.

## 2. Spatially Resolved Ion Beam Characterization Diagnostic

A simplified diagram of the target is shown in Fig. 1. The central target was a gold cone of 0.5- or 1-micron-thick gold with a 19 $^{o}$ half-angle, resting on a Parylene-D support structure. TPX foam (polymethyl pentene) of 3 or 6 mg/cm$^3$ filled the cone. The ends of the cone were left open for diagnostic access for all but three shots. In these three targets, the narrow ends were enclosed with the same thickness of gold as the sides, and the wider end was enclosed with a 1-μm-thick layer of gold which had a 3-mm-diameter aperture in the center. The conical shape allowed the ion-beam parameters to be determined by the diagnostics viewing ion-induced x-ray fluorescence from the bottom of the target. In addition, the conical shape provided access for the thermal x-ray diagnostics to view the target and make measurements of thermodynamic motion.[5]

A 1-mm-wide aluminum strip coated with 2 microns of titanium is placed near the gold cone for characterization of the beam, as shown in Fig. 1. The strip makes a 60 degree angle with the horizontal with a midplane radius of 10 mm from the diode axis. Titanium $K_\alpha$ fluorescence at 4.5 keV generated by ion impact of incident beam on the titanium strip was used to reconstruct the

beam profile on the strip. The $K_\alpha$ inner-shell fluorescence was . The strip was narrow enough to not subtend a significant amount of beam (of order 2%), but wide enough to provide a beam profile at one azimuthal angle. The strip was thick enough to preclude ion beam fluorescence from other azimuthal angles (such as from the opposite side of the anode at 180° from passing through the strip).

Previous PBFA II target shots[5] included an Ar-filled gas cell near the target to allow for ballistic focussing of the ion beams near the target. However, difficulties in target fabrication required a design that included vacuum transport for the final 1.4 cm of the ion trajectory before intercepting the target. This vacuum-transport region appeared to play a role in target focus.

The ion beam characterization discussed in this paper was performed from film images acquired with the time-integrated x-ray pinhole cameras (TIXRPHCs) fielded below the PBFA II diode (see Fig. 2). These cameras viewed the target assembly from below at an 8° angle from the vertical axis passing through the cone axis. X-ray images of the targets were recorded on selectively filtered film plates. We viewed the titanium strip with a TIXRPHC filtered for Ti $K_\alpha$ (4.5 keV) characteristic line radiation and the gold cone with a TIXRPHC filtered for Au $L_\alpha$ (9.65 keV) or Au $M_\alpha$ (2.1 keV) characteristic line radiation. Both Kodak direct exposure film (DEF) and SB-5 film were used.[6] The camera film and filter pack was 95 cm from the target with a magnification factor of 0.69. Magnets placed at the pinhole swept away any ions that Rutherford-scatter into the camera line-of-sight, eliminating ion contamination of the film images.[7] Appropriate shielding eliminated a majority of the bremsstrahlung created from the electron loss in the vacuum feed of the diode region.[8] The remaining bremsstrahlung formed a uniform background on the film images that was well below film saturation. The film was developed using guidelines from B. L. Henke,[9-11] converting from net film density to either the inferred Au $L_\alpha$, Au $M_\alpha$, or Ti $K_\alpha$ intensity (similar to the procedure used in proton beam experiments discussed in Ref. 12). For these x-ray lines, the image is preferentially weighted towards higher lithium ion energies, seen at the beginning of the voltage pulse and spanning the time of peak power in the incoming beam. We made no correction for filter transmission per se since the parameters we seek depend on relative, rather than absolute, intensities.

## 3. Results

To reconstruct the ion beam vertical profiles, I(z), from the titanium strip image, we factored in a 1/r radial correction due to the radial focus of the ion beam focus to the center axis of the diode. Assuming that beam focus is a function of radius, the current density J(r) is a function of radius. Each radius on the image corresponds to axial position of the beam. Since J(r) is distributed over a smaller differential area ($2\pi r\delta z$) as the titanium strip radius from the target center decreases, J(r) is weighted towards small values of r. To get relative axial intensity I(z), a radial correction $I(r) = J(r)2\pi r$ and a transformation to the vertical distance z above or below the target's midplane using a simple $\tan\theta$ geometrical transformation was applied. The radial position of the titanium strip at the target midplane was a nominal 10 mm from the central axis of the diode. From these beam profiles, we determined the lithium beam's centroid position above or below the target midplane and the lithium beam's FWHM. In cases of a wide beam or a beam where the centroid is displaced from the target midplane and the full beam profile cannot be resolved, twice the half-width-at-half-maximum was used to calculate the FWHM. Not all shots had adequate intensity on target for analysis. On the beam profiles of these shots (with the exception of shots # 5975 and # 5979), the intensity of observed sharp edges decreased to half-maximum within 0.8 mm to 1.5 mm (varying shot-to-shot), indicating that the contrast resolution of the cameras was nominally $\pm$ 1 mm at the target. For the two shots mentioned as exceptions, the resolution was considerably worse.The results of the vertical beam profile analysis from the titanium strips are summarized in Table 1.

Two shots with comparable targets had sufficient Au $L_\alpha$ yield for beam intensity analysis. We could then obtain vertical beam profiles at two different radial positions along the same azimuthal direction from the gold cone and titanium strip. The data comparing the Au cone beam parameters at an average 3 mm from the center axis of the diode at the target midplane with that of the titanium strip beam parameters measured at 10 mm are shown in Table 2a.

For shots 5936 and 6000, the azimuthal variation in beam-induced fluorescent intensity along the gold cone midplane was measured. For these midplane intensity profiles, four points in the center of the four quadrants of the cone were used to estimate azimuthal intensity. The same angles with respect to north were used in each case. Corrections to the spot intensities due to the TIXRPHCs $8^\circ$ tilt were taken into account. The mean and standard deviations of the four intensities for each shot were calculated and are shown in Table 2b. Albeit a rough measure, the standard deviations were 24% and 30% of the mean for shots 5936 and 6000. These numbers are roughly comparable to the azimuthal asymmetries found for previous proton target shots.[13]

It is evident from these data that beam steering problems occurred during this lithium beam series.[12] There is evidence that the lithium beam intensity at 10 mm and 3 mm radii varied in a way which suggests beam instabilities or focussing problems with the beam near the target. The centroid's vertical position at 10 mm for both these shots was slightly below the target midplane. But at the gold foil position at 3 mm, the centroid's position was quite high. For shot 6000, the ion beam intensity is still increasing at the upper edge of the cone, making it impossible to measure a beam FWHM, but indicating still a beam centered above the target midplane.

From these measurements, we have demonstrated that variations in lithium beam focus and symmetry can be characterized during lithium beam target shots of sufficient intensity with our x-ray cameras. The relative quality of the focus and figures of merit for the ion beam (FWHM, vertical centroid position, azimuthal symmetry) were obtained for the higher intensity shots that are of interest. Future shots will allow us to build a more extensive data base of the ion beam behavior during target experiments. The reasons for the variation in beam position, width, symmetry, and overall shot-to-shot reproducibility are actively being investigated.

## 4. Future Work

The next target series will utilize cylindrical targets designed to optimize target temperature. To maximize the hohlraum temperature, the target geometry will be modified from a conical gold shell to a cylindrical gold shell. The beam characterization diagnostics must be modified since the target surface cross section will not provide an inner-shell x-ray image with the diagnostic setup used previously. Because of the lithium ion range, past solutions to this problem, such as using a large radius gold cone as used in past proton beam series, would seriously degrade lithium beam energies and is not an option for these experiments. To obtain information on the beam azimuthal symmetry, an expanded beam diagnostic - dubbed the titanium "bird cage" will be fielded on this upcoming target series. A set of 3 to 5 solid titanium strips of 0.5 mm width will be fielded in a skeletal cone about the inner target, producing an ion beam profile similar to the last experiment at the 3 to 5 azimuthal angles about the cylindrical inner target. We will then be able to obtain vertical focus and width in separate quadrants, gain a more complete measurement of azimuthal symmetry, and add to the shot-to-shot reproducibility data base.

This work supported by the U. S. Department of Energy under Contract No. DE-AC04-94-AL85000.

## References


[1]J. P. VanDevender and D. L. Cook, Science **232**, 837 (1986).

[2]D. L. Cook *et al.*, Plasma Phys. Controlled Fusion **28**, 1921 (1986).

[3]D. J. Johnson, T. R. Lockner, R. J. Leeper, J. E. Maenchen, C. W. Mendel, G. E. Rochau, W. A. Stygar, R. S. Coats, M. P. Desjarlais, R. P. Kensek, T. A. Mehlhorn, W. E. Nelson, S. E. Rosenthal, J. P. Quintenz, and R. W. Stinnett, Proc. of the 7th IEEE Pulsed Power Conference, Monterey, CA, 1989, p. 944.

[4]D. J. Johnson, Sandia National Laboratories, private communication (1994).

[5]G. A. Chandler, J. Aubert, J. Bailey, A. Carlson, D. Derzon, M. Derzon, R. Dukart, R. Humphreys, J. Hunter, D. J. Johnson, M. K. Matzen, A. R. Moats, R. Olson, J. Pantuso, P. Rockett, C. Ruiz, P. Sawyer, J. Torres, and T. Hussey, Rev. of Sci. Instrum. **63** (10), 4828 (1992).

[6]W. C. Phillips and G. N. Phillips, Jr., J. Appl. Crystallogr. **18**, 3 (1985).

[7]A. R. Moats and T. A. Mehlhorn, Rev. of Sci. Instrum. **61** (10), 2792 (1990).

[8]M. S. Derzon, M. A. Sweeney, P. Grandon, H. C. Ives, R. P. Kensek, L. P. Mix, and W. A. Stygar, Rev. Sci. Instrum. **59**, 1834 (1988).

[9]B. L. Henke, J. Y. Uejio, G. F. Stone, C. H. Dittmore, and F. G. Fujiwara, J. Opt. Soc. Am. Bull. **3**, 1540 (1986).

[10]B. L. Henke, S. L. Kwok, J. Y. Uejio, H. T. Yamada, and G. C. Young, J. Opt. Soc. Am. Bull. **1**, 818 (1984).

[11]B. L. Henke, F. G. Fujiwara, and M. A. Tester, J. Opt. Soc. Am. Bull. **1**, 828 (1984).

[12]M. S. Derzon, G. E. Rochau, G. A. Chandler, A. R. Moats, R. J. Leeper, "Shot-to-Shot Comparison of the First Lithium Beam Hohlraum Results," these proceedings.

[13]A. R. Moats, M. S. Derzon, D. J. Johnson, W. E. Nelson, J. G. Pantuso, C. L. Ruiz, and D. F. Wenger, Rev. of Sci. Instrum. **63** (10), 5065 (1992).

| Shot No. | Au cone wall - thickness (mm) | CH Foam Density (mg/cc) | Closed/ Open geometry | Centroid z (mm) | FWHM (mm) | Comments |
|---|---|---|---|---|---|---|
| 5936 | 1.03 ± 0.01 | 4.75 ± 0.05 | Open | -1.2 ± 1.1 | 12.0 ± 1.1 | |
| 5942 | 0.49 ± 0.01 | 4.75 ± 0.05 | Open | -1.2 ± 1.2 | >8.2 | Slight defect in Ti strip made FWHM measure difficult. |
| 5975 | 1.04 ± 0.01 | 2.38 ± 0.05 | Closed | -2.7 ± 2.9 | 9.7 ± 2.9 | |
| 5979 | 1.01 ± 0.01 | 2.38 ± 0.05 | Closed | +0.3 ± 2.9 | >12.0 | Beam broader than Ti strip |
| 6000 | 0.99 ± 0.01 | 4.75 ± 0.05 | Open | -1.2 ± 0.8 | 11.5 ± 0.8 | |
| 6010 | 0.51 ± 0.01 | 4.75 ± 0.05 | Open | +0.7 ± 1.5 | 5.9 ± 1.5 | Signal/ noise very low |

Table 1. The vertical beam profiles above were obtained from analysis of the titanium strip (Ti $K_\alpha$), yielding the centroid vertical focus and the full-width-at-half-maximum (FWHM). These time-integrated x-ray pinhole camera measurements are at a nominal 10 mm radius from the center of the target. Uncertainties were measured from sharp-edge contours on the film images. The target midplane is at z=0 mm. Shots not shown were of low intensity.

| Shot No. | 5936 | 6000 | Comments |
|---|---|---|---|
| Au cone centroid position (z in mm) | +2.0 ± 1.8 | > 3.0 | This is location of the centroid of the focus above target midplane at a radius of 3 mm from diode center, same azimuth as Ti strip. |
| Ti strip centroid position (z in mm) | -1.2 ± 1.1 | -1.2 ± 0.8 | This is focus below target midplane at a radius of 10 mm from diode center, same azimuth as Au cone measurement. |
| Au cone FWHM (mm) | 7.8 ± 1.8 | undefined | At 3 mm from center, same azimuth as Ti strip. |
| Ti strip FWHM (mm) | 12.0 ± 1.1 | 11.5 ± 1.3 | At 10 mm from center, same azimuth as Au cone. |

Table 2a. Ion beam focus and width as a function of radius from center (at the Ti strip and Au cone radii) are compared in the table above.

| Shot No. | 5936 | 6000 | Comments |
|---|---|---|---|
| Mean midplane intensity (relative units) | 3.6 | 5.2 | Intensity along Au cone midplane, using Au $L_\alpha$ intensity. This is at approximately 3 mm from diode center. Mean was calculated at four points, one in each quadrant. |
| $\sigma$ of midplane intensity (relative intensity) | 1.1 | 1.2 | Calculated from the four measurements, one in each cone quadrant, per shot. |
| $\sigma$ (as % of mean) | 30.4 | 24.0 | |

Table 2b. For the two shots #5936 and #6000 shown above, the Au $L_\alpha$ deviation in intensity with azimuthal angle along the midplane of the target Au cone was measured.

Figure 1. Sketches (not to scale) of the central lithium-ion beam target. (a) Side-view of the gold cone, showing the titanium strip at 10 mm radius at the cone midplane, and the three aluminum and one titanium current-return wires at the bottom of the cone. The 1 micron coating of Parylene_D was used as a support structure. (b) Bottom-view of the central target. Compare this with the image in Figure 2.

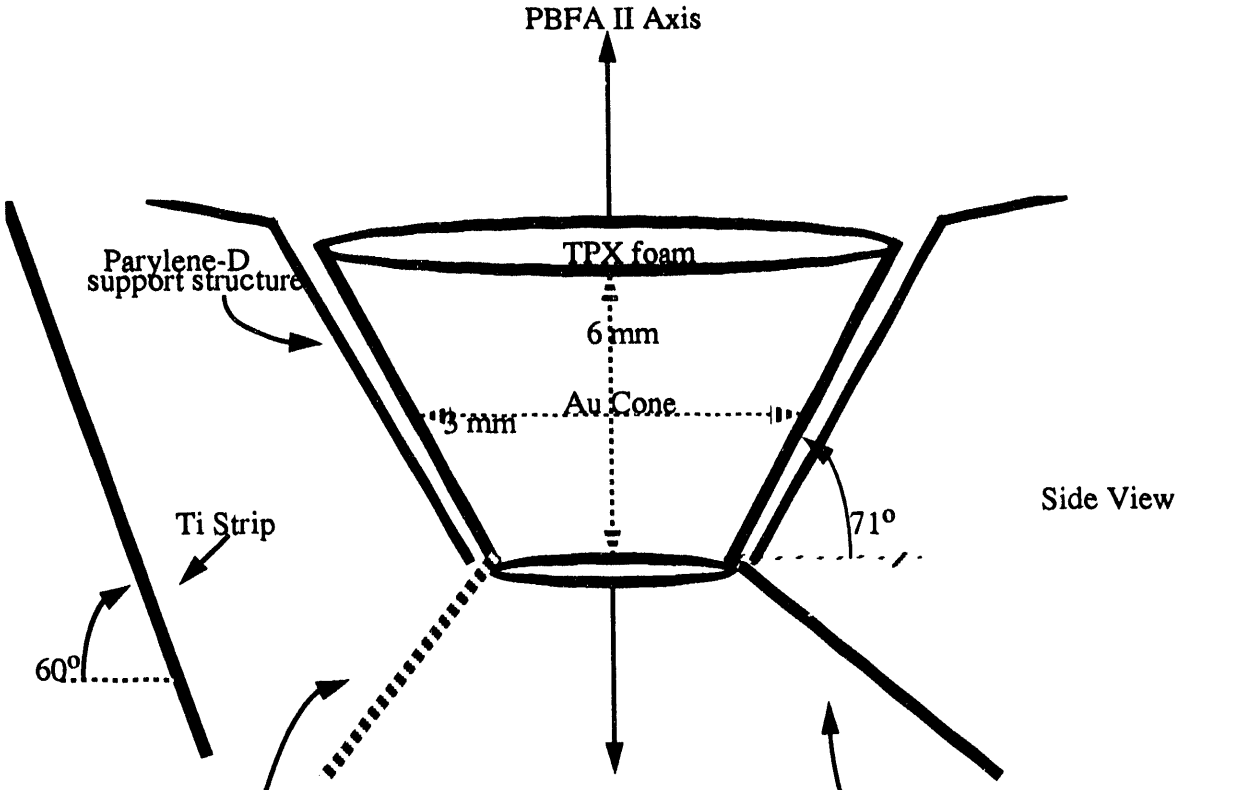


Figure 1a.

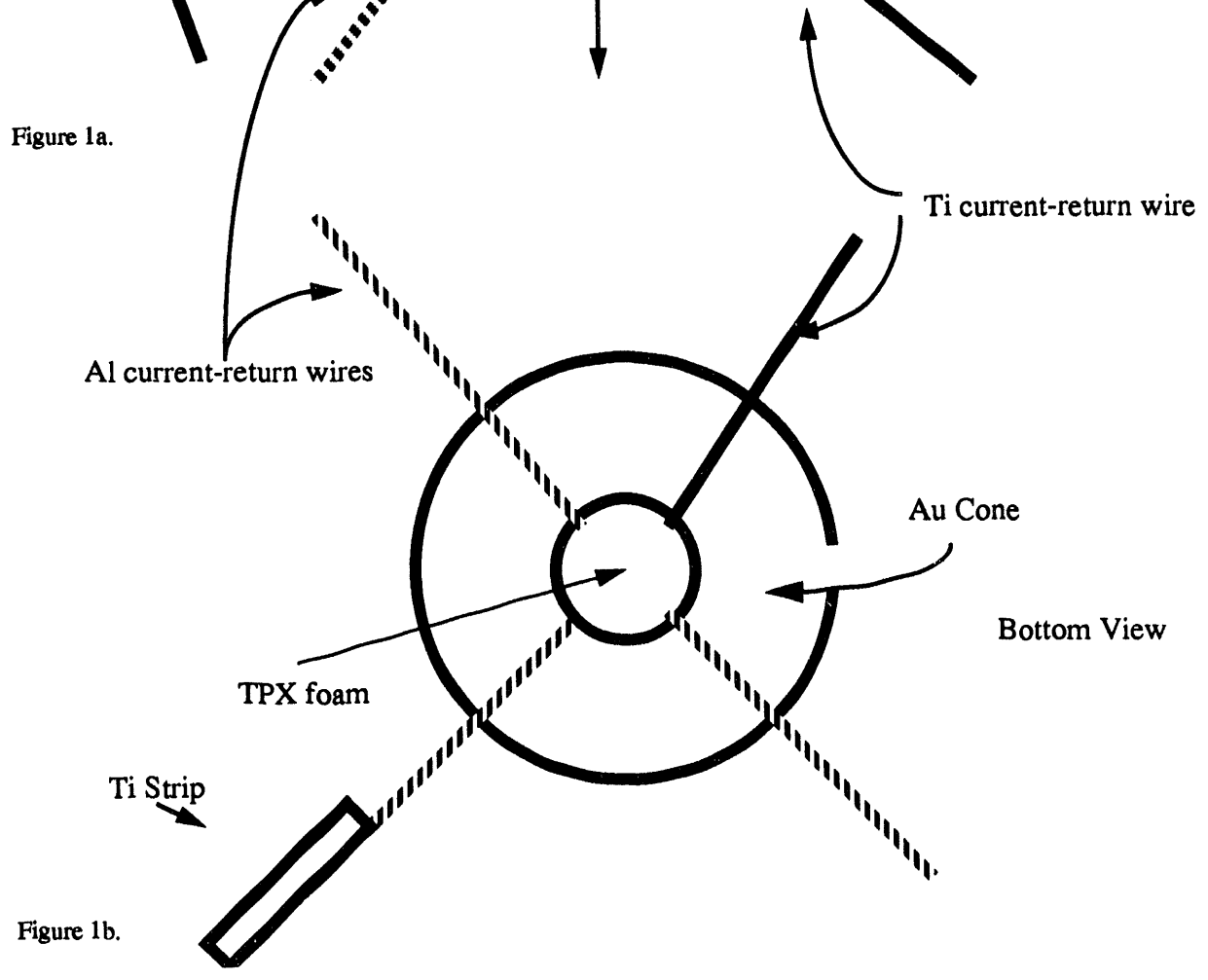


Figure 1b.

Figure 2. The relative intensity image of the central target region. The titanium strip, the cone target, and the titanium current-return wire are shown in a view tilted $8^{o}$ from the central axis of symmetry and imaged along a line-of-sight from below the target region. The spectral region around 4.5 keV (Ti $K_{\alpha}$) is shown on this TIXRPHC image. The brighter region on the right-hand side of the gold cone is due to the $8^{o}$ tilt angle. The appearance of lobes in the image is due to the shadowing from target-holder posts. The gold cone is observed because of a substantial Au $L_{\alpha}$ sensitivity for the camera response.

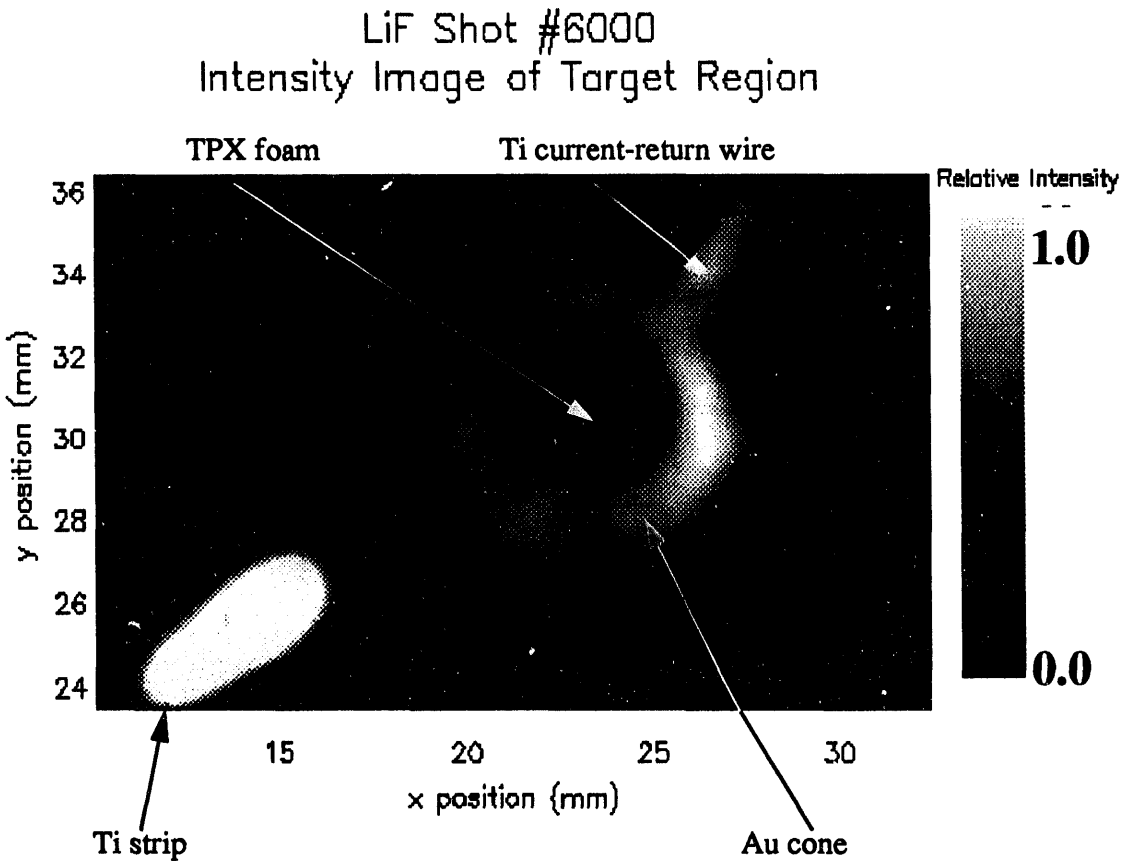
LiF Shot #6000
Intensity Image of Target Region
TPX foam
Ti current-return wire
Relative Intensity
1.0
0.0
36
34
32
30
28
26
24
y position (mm)
15
20
25
30
x position (mm)
Ti strip
Au cone

DATE
FILMED
6/29/94
END